Supporting Information

Impacting pancreatic cancer therapy in heterotypic *in vitro* organoids and *in vivo* tumors with specificity-tuned, NIR-activable photoimmuno-nanoconjugates: towards conquering desmoplasia?

Girgis Obaid,[a] Shazia Bano,[a] Srivalleesha Mallidi,[a] Mans Broekgaarden,[a] Jerrin Kuriakose,[a] Zachary Silber,[a] Anne-Laure Bulin,[a] Yucheng Wang,[a] Zhiming Mai,[a] Wendong Jin,[a] Diane Simeone[b] and Tayyaba Hasan[a][c]*

[a] Wellman Center for Photomedicine, Massachusetts General Hospital and Harvard Medical School, Boston, Massachusetts 02114, U.S.

[b] Department of Surgery and Department of Pathology, Perlmutter Cancer Center, New York University Langone Health, New York City, New York 10016, U.S.

[c] Division of Health Sciences and Technology, Harvard University and Massachusetts Institute of Technology, Cambridge, Massachusetts 02139, U.S.

KEYWORDS: nanoengineering, photoimmuno-nanoconjugates, pancreatic ductal adenocarcinoma, NIR photodynamic activation, heterotypic organoids

MATERIALS AND METHODS

Site-specific Protein Z-N_3 conjugation to cetuximab: An azido moiety was site-specifically introduced to the Fc region of cetuximab through a photocross-linked recombinant Protein Z (Pz) intermediate, tethered to a terminal azido fluorescent peptide (FP-N_3). The Pz-FP-N_3 construct, referred to as Pz-N_3 from hereon, was covalently tethered to cetuximab's (Cet) Fc region by the photocross-linking of benzoylphenylalanine (BPA), engineered into the IgG binding domain of the recombinant Pz. The expression, isolation and site-specific photocross-linking of Pz-N_3 to Cet of Pz-N_3 was as described below.

a) expression of Pz: Pz containing the unnatural amino acid photocross-linker, benzoylphenylalanine (BPA,) at the IgG binding site was expressed as previously described.[1] Briefly, T7 Expression Crystal Competent Cells (New England Biolabs, Ipswich, MA) cotransformed with a pEVOL-pBpF plasmid (Addgene, Cambridge, MA) encoding the BPA incorporation machinery and the pSrtA-Pz plasmid (Integrated DNA Technologies, Coralville, IA) encoding the Sortase-Pz construct were cultured overnight at 37°C on agar plates containing ampicillin (250 μg/ml; Thermo Fisher Scientific) and chloramphenicol (100 μg/ml; Thermo Fisher Scientific). The cells were a kind gift from Dr. Andrew Tsourkas, University of Pennsylvania. Cloning of the Pz fusion protein vector was performed as previously described.[2] Ampicillin and chloramphenicol selects for cells expressing both Pz and pEVOL-BPA, respectively. Ampicillin (100 μg/ml final concentration) and chloramphenicol (25 μg/ml final concentration) were added to Overnight Express™ Autoinduction media (AI media, 100 ml; EMD Milipore) supplemented with Ampicillin (100 μg/ml), chloramphenicol (25 μg/ml). Arabinose (10% stock in water; Thermo Fisher Scientific) was added to the AI media at a 1:100 dilution to induce pEVOL-BPAx. 4-benzoyl-L-phenylalanine (BPA, 10 mM stock in 100 mM NaOH; Alfa Aesar) was added to the AI media at a 1:300 dilution). A single colony from the co-transorfmed T7 Expression Crystal

Competent Cells cultured on the agar plates was inoculated into the AI media prepared. The cells were grown at 37°C and monitored at 600nm to obtain an OD of 0.4-0.6. Isopropyl β-D-1-thiogalactopyranoside (IPTG, 500 mM stock in water; Thermo Fisher Scientific) was added to the cells cultured in AI media at a 1:1000 dilution to induce protein expression. The cells were allowed to express for 48 h at 37°C. The cells were centrifuged at 5,500 xg for 7 min, the supernatant was aspirated and the cell pellets were lysed with Bacterial Protein Extraction Reagent (B-PER; Pierce) containing EDTA-free protease inhibitor tablets (Roche) at a ratio of 1 g cell pellet to 4 ml B-PER reagent. The cells were incubated for 20 min at room temperature in the B-PER reagent, then sonicated for 15 cycles of 5s pulses using a Fisher Sonic Dismembrator Model 300 sonicator operating at 40%. Following each pulse, the cell lysates were cooled on ice. The lysate was centrifuged at 10,000 xg at 4°C for 10 min in a microcentrifuge tubes to pellet insoluble cell debris.

b) Isolation of Pz-azido fluorescent peptide (Pz-N_3): TALON® Metal Affinity slurry (2 ml; Clontech) was packed into 10 ml poly-prep columns (Bio-Rad Laboratories, Inc.), washed once with 8 ml Milli-Q® water and twice with 8 ml 1x DPBS (no calcium or magnesium, Corning®). The stopper was attached to the column, the pooled clarified bacterial supernatant was loaded onto the column and the column was capped. The column was then orbitally rotated at room temperature for 30 min in the dark to allow the expressed his-tag fusion protein to bind to the resin. The flow-through was then drained from the column and the column was washed three times with 8 ml 1x DPBS. The column was then loaded with the custom triglycine azido fluorescent peptide (1 ml, 200 μM in 1x DPBS, 1030 g/mol; AnaSpec Inc.) with calcium chloride dihydrate (50 μM, 147.01 g/mol; Sigma-Aldrich) and the stopper was attached to the column. The custom made heterobifunctional azido fluorescent peptide sequence (NH_2-Gly-Gly-Gly-Lys(5-FAM)-Gly-Gly-Ser-Lys(N_3)-NH_2)[1] contains a triglycine sequence to mediate sortase cleavage and conjugation to

Pz, a fluorescent 5-FAM molecule for quantitation and a terminal azide to mediates click conjugation to PINs. The resin was mixed to evenly distribute the peptide and calcium chloride, and the column was incubated for 6 h at 37°C to allow for sortase cleavage and peptide ligation to Pz. The cleaved Pz-azido fluorescent peptide conjugate (Pz-N_3) was eluted from the column using 2 ml 1x DPBS and analyzed using denaturing SDS-PAGE. The Pz-N_3 was lyophilized and each 100 ml culture equivalent of lyophilized Pz-N_3 was reconstituted in 100 µl of Milli-Q® water. The Pz-N_3 concentration was determined using the 5-FAM absorbance ($\varepsilon_{492\ nm}$ = 82,000 $M^{-1}.cm^{-1}$), which exists at a 1:1 ratio when the peptide is tethered to the Pz. The Pz-N_3 was then stored at 4°C in the dark until site-specific photo-crosslinking to Cet.

c) Site-specific photo-crosslinlking of Pz-N_3 to Cet: Pz-N_3 was mixed with Cet (2 mg/ml in 1x DPBS, 145781.6 g/mol (FASTA sequence analysis), Erbitux®; Ely Lily) at a 3:2 molar ratio in 1 h at room temperature in the dark to allow for the site-specific non-covalent binding Pz-N_3 to the Cet Fc region. The Cet-Pz-N_3 complex was placed in transparent 96 well multidishes in 100 µl aliquots and irradiated at 365 nm for 90 min on ice using a 115V Handheld LW 6W UV lamp (UVL-56; UVP). The UV-irradiated Cet-Pz-N_3 mixture was then buffer exchanged with glycine-HCl buffer (200 mM, pH 3.5) by centrifugation in a 30 kDa ultrafiltration tube (EMD Millipore) at 5,000 xg for 5 min at 4°C then incubated in the dark at room temperature for 10 min to allow the dissociation of non-covalently bound Pz-N_3. The Cet-Pz-N_3 mixture in glycine-HCl buffer was then loaded onto a 10 mL borosilicate Poly-Prep chromatography column (Bio-Rad) packed with Superdex 75 prep grade (GE Healthcare Life Sciences), equilibrated with 1x DPBS using a syringe pump at a flow rate of 0.05 ml/min. The higher molecular weight fraction consisting of the photo-crosslinked Cet-Pz-N_3 was collected and concentrated by centrifuging in 30 kDa ultrafiltration tubes (EMD Milipore) at 2,500 xg for 20 min at 4°C. UV-Visible spectrophotometry was used to

determine the concentration of Cet ($\varepsilon_{280\ nm}$ = 217,315 $M^{-1}.cm^{-1}$ (Expasy ProtParam Tools))[3] and 5-FAM present corresponding to the Pz-AzFP photocross-linked to the cetuximab ($\varepsilon_{492\ nm}$ = 82,000 $M^{-1}.cm^{-1}$). The purified Cet-Pz-N_3 was stored in the dark at 4°C until needed for click conjugation to the PINs.

Stochastic NHS-PEG_4-N_3 conjugation to Cet: An azido moiety was stochastically introduced to Cet through the conjugation of N-hydroxysuccinimidyl azido poly(ethylene glycol)4 (NHS-PEG_4-N_3, 388.37 g/mol; Thermo Fisher Scientific) to the antibody's lysine residues. Cet was also conjugated to the N-hydroxysuccinimidyl ester of Alexa Fluor® 488 (AF488-NHS, 643.4 g/mol; Thermo Fisher Scientific). Stock solutions of NHS-PEG_4-N_3 (10 mg/ml) and AF488-NHS (1 mg/ml) in anhydrous dimethyl sulfoxide (DMSO; Sigma-Aldrich) were mixed at quantities corresponding to a 2.5-fold molar excess of each molecule to Cet prior to addition of the antibody. Cet (2 mg/ml in 1x DPBS) was then added to the NHS-PEG_4-N_3 and AF488-NHS mixture and was mixed by orbital rotation for 24 h at 4°C. Unreacted NHS-PEG_4-N_3 and AF488-NHS were removed from the conjugated cetuximab by illustra NAP Columns (GE Healthcare Life Sciences) equilibrated with 1x DPBS. The purified Cet conjugated to both AF488 and PEG_4-N_3 (Cet-PEG_4-N_3) was collected and concentrated by centrifuging in 30 kDa ultrafiltration tubes (EMD Milipore) at 2,500 xg for 20 min at 4°C. UV-Visible spectrophotometry was used to determine the concentration of Cet ($\varepsilon_{280\ nm}$ = 217,315 $M^{-1}.cm^{-1}$ (information obtained using Expasy Protoparam Tools))[3] and Alexa Fluor® 488 ($\varepsilon_{494\ nm}$ = 71,000 $M^{-1}.cm^{-1}$ (Invitrogen™ Manual MAN0002151)). The purified Cet-PEG_4-N_3 was stored in the dark at 4°C until needed for click conjugation to the nanoconstructs. 1.07 PEG_4 azide molecules were conjugated to each Cet molecule, as validated using a 10x reaction with Cy5-DBCO ($\varepsilon_{650\ nm}$ = 250,000 $M^{-1}.cm^{-1}$) and purification with Sephadex G25 (superfine) size exclusion chromatography.

Denaturing gel electrophoresis of Cet-Pz and Cet-PEG$_4$-N$_3$: Free Cet, Cet-Pz and Cet-PEG$_4$-N$_3$ in PBS were denatured with mercaptoethanol, loaded onto Mini-PROTEAN TGX (Bio-Rad) 4-20% acrylamide gels and then ran for 1 h with Precision Plus Protein™ Dual Xtra Standards (Bio-Rad). The gels were removed from the cassettes and soaked in GelCode™ Blue Safe Protein Stain (Thermo Fisher Scientific) for 20 min in the dark. The gels were then de-stained in multiple Milli-Q® water washes and imaged using a Gel Logic 200 Imaging System (Kodak).

Synthesis of the BPD conjugates of 16:0 lyso PC and 20:0 lyso PC: The carboxylate of the benzoporphyrin derivative photosensitizer was coupled to the hydroxyl moiety of the phospholipid 1-palmitoyl-2-hydroxy-sn-glycero-3-phosphocholine (16:0 lyso PC) using Steglich esterification, according to an adaptation of a previously reported protocol for porphyrins[4] and directly as reported previously by our group.[5] Briefly, the following constituents were mixed at a 1 : 5 : 50 : 25 : 300 molar ratio, respectively: 16:0 lyso PC (495.63 g/mol, chloroform; Avanti® Polar Lipids, Inc.), benzoporphyrin derivative monoacid ring A (BPD, verteporfin, mixed isomers, 718.79 g/mol; U.S. Pharmacopeia (USP®)), 1-ethyl-3-(3dimethylaminopropyl) carbodiimide (EDC, 155.24 g/mol; Sigma-Aldrich), 4-(dimethylamino)pyridine (DMAP, 122.17 g/mol; Sigma-Aldrich), and *N,N*-Diisopropylethylamine (DIPEA, 129.24 g/mol. 0.742 g/ml; Sigma-Aldrich). The mixture was dissolved in dichloromethane (DCM, 5 ml, ACS Reagent Grade, 99.5%; Sigma-Aldrich) and rigorously stirred at 2500 RPM for 72 h at room temperature in the dark using a magnetic stir plate. The 16:0 lyso PC-BPD lipid conjugate (16:0 BPD-PC) was purified using Analtech Preparative Thin Layer Chromatography Silica Uniplates (Sigma-Aldrich) running on a mobile phase consisting of 10% methanol in DCM. The 16:0 BPD-PC-containing silica fraction (Rf = 0.144) was removed from the TLC plate and the conjugate was extracted by sonication in 33% methanol in DCM for 10 min. The silica was sedimented by centrifugation at 3,700 xg for 10

min and the supernatant containing the extracted 16:0 BPD-PC was collected into a round-bottom flask. The silica fraction was washed two further times and all 16:0 BPD-PC solutions were pooled into the round bottom flask. The solvent mixtures were removed from the extract by rotary evaporation under reduced pressure at 40°C connected to a liquid nitrogen trap condenser. Residual silica previously solubilized in the 33% methanol in DCM solvent mixture was removed by redissolving the dried 16:0 BPD-PC extract in pure DCM. The insoluble silica precipitate was removed by filtration using a Fisherbrand™ poly(tetrafluoroethylene) (PTFE) filter (0.22 μm pore size, 13 mm diameter; Thermo Fisher Scientific) driven by a gastight glass syringe. The DCM was removed from the filtered 16:0 BPD-PC solution using rotary evaporation as described and the purified conjugate was redissolved in chloroform and stored in the dark at -20°C. The concentration of the 16:0 BPD-PC was determined by diluting the phospholipid conjugate in DMSO and measuring the UV-Visible absorption spectrum using $\varepsilon_{687\ nm}$ = 34,895 $M^{-1}.cm^{-1}$. The lysophospholipid 1-arachidoyl-2-hydroxy-*sn*-glycero-3-phosphocholine (20:0 lyso PC) was conjugated to BPD using the same procedure. All lipidated BPD variants were validated with MALDI using 3,4-dihydroxybenzoic acid (10mg/ml in ethanol; Sigma Aldrich) as a matrix. The expected M.W. of 16:0 BPD-PC (99.02% purity) is 1196.41 g/mol, the observed M.W. is 1197.123 m/z. The expected M.W. of 20:0 BPD-PC (95.52% purity) is 1252.52 g/mol, the observed M.W. is 1255.715 m/z. Purity was assessed using HPLC with a gradient of 95/5 water/acetonitrile (0.1% TFA) to 5/95 water/acetonitrile (0.1% TFA) over 30 minutes, followed by a 30 minute hold at 5/95 water/acetonitrile (0.1% TFA).

Synthesis of the BPD conjugate of DSPE-PEG$_{2000}$-NH$_2$: BPD was conjugated to DSPE-PEG$_{2000}$-NH$_2$ using EDC amide coupling as described previously.[5] Briefly, DSPE-PEG$_{2000}$-NH$_2$ in chloroform was mixed with a 10-fold molar excess of BPD and a 5-fold molar excess of EDC to

BPD in a 13 x 100 mm Pyrex® tube. The mixture was stirred in the dark at 2500 RPM for 72 h. The chloroform was then evaporated using a flow of nitrogen and the dry reaction mixture was dissolved in 1ml methanol. The reaction mixture was then run through Sephadex® LH-20 (GE Healthcare Life Sciences) equilibrated with methanol, and the fastest running colored fraction consisting of DSPE-PEG_{2000}-BPD was collected. The methanol was evaporated and the DSPE-PEG_{2000}-BPD was dissolved in chloroform and stored in the dark at -20°C. The concentration of the DSPE-PEG_{2000}-BPD was determined by diluting the conjugate in DMSO and measuring the UV-Visible absorption spectrum using using $\varepsilon_{687\ nm}$ = 34,895 $M^{-1}.cm^{-1}$. The DSPE-PEG_{2000}-BPD conjugate (97.27% purity) was validated with MALDI as described earlier. The expected M.W. is 3479.25 g/mol and the observed M.W. is 3588.481 m/z. This discrepancy is due to the normal distribution of all PEG chain lengths conjugated to DSPE.

Nanoconstruct synthesis: All nanoconstruct liposomal-based formulations were prepared using the hydrated lipid film process. Lipid films were prepared in 13 x 100 mm Pyrex® tubes using chloroform solutions of 1,2-dipalmitoyl-sn-glycero-3-phosphocholine (DPPC, 734.04 g/mol), 1,2-dioleoyl-3-trimethylammonium-propane (chloride salt) (DOTAP, 698.54 g/mol) *OR* 1,2-dioleoyl-*sn*-glycero-3-phospho-(1'-*rac*-glycerol) (sodium salt) (DOPG, 797.026 g/mol), cholesterol (386.65 g/mol), 1,2-distearoyl-sn-glycero-3-phosphoethanolamine-N-[methoxy(polyethyleneglycol)-2000] (ammonium salt) (DSPE-$mPEG_{2000}$, 2805.50 g/mol) and 1,2-distearoyl-sn-glycero-3-phosphoethanolamine-N-[dibenzocyclooctyl(polyethylene glycol)-2000] (ammonium salt) (DSPE-PEG_{2000}-DBCO, 3077.80 g/mol), all purchased from Avanti® Polar Lipids, Inc. DPPC, DOTAP/DOPG, cholesterol, DSPE-$mPEG_{2000}$ and DSPE-PEG_{2000}-DBCO were mixed at a molar ratio of 0.582 : 0.079 : 0.289 : 0.045 : 0.005, respectively. PEGylated DSPE was consistently kept at a total of 5mol %, with 0.5 mol% substituted for DSPE-PEG_{2000}-DBCO to mediate the copper-

free click conjugation to azide-derivatized antibodies and targeting moieties. The BPD or its lipidated variants (16:0 BPD-PC, 20:0 BPD-PC, cholesterol-BPD or DSPE-PEG_{2000}-BPD), were introduced to the lipid mixture at 0.6 mol%, replacing their respective DPPC molar fraction. All lipids were briefly vortexed (Fisher Scientific™ Analog Vortex Mixer) and the chloroform was evaporated using a flow of nitrogen gas through a 16-gauge needle with continuous rotation to form the thin lipid film. Residual chloroform was removed by storing the lipid film under vacuum overnight. The dried lipid film was hydrated in 1x DPBS (1 ml; Corning®) using 5 cycles of the freeze-thaw-vortex method by incubating in a darkened water bath at 42°C for 10 min, vortexed for 30 s, then incubated in ice for 10 min. To prepare monodisperse unilamellar liposomal nanoconstructs, the lipid suspensions were extruded 11 times at 42°C through two polycarbonate membranes, (0.1 μm pore size, 19 mm diameter; Avanti® Polar Lipids, Inc.) using an Avanti® Mini-Extruder kit. The nanoconstructs were stored at 4°C in the dark. The concentration of the BPD variants within the nanoconstruct formulations was determined using UV-Visible absorption spectroscopy ($\varepsilon_{687\ nm}$ = 34,895 $M^{-1}.cm^{-1}$) in DMSO dilutions. The majority of the nanoconstructs were prepared using 16:0 BPD-PC, which will be referred to as BPD-PC from hereon for simplicity. The expermients measuring the photobleaching of BPD nanoconstructs and BPD-PC nanoconstructs were performed in 1xPBS in black-walled, transparent base 96 well plates (Thermo Fisher Scientific) irradiated with 690 nm light at an irradiance of 150 mW/cm^2.

Site-specific (Cet-Pz-N_3) and stochastic (Cet-PEG_4-N_3) cetuximab nanoconstruct conjugation using copper-free click chemistry: Both Cet-Pz-N_3 and Cet-PEG_4-N_3 in 1x DPBS were reacted with the BPD-PC nanoconstructs at lipid : Cet mass ratios of 1:0.02, 1:0.05, 1:0.1, 1:0.15 or 1:0.2 and incubated at room temperature for 24 h with continuous orbital rotation. Following copper-free click conjugation of surface DSPE-PEG_{2000}-DBCO to the azide moieties site-specifically (Cet-Pz-

N_3) or stochastically (Cet-PEG_4-N_3), unbound antibody was removed from the nanoconjugates using 10 mL borosilicate Poly-Prep chromatography columns (Bio-Rad) packed with Sepharose CL-4B (Sigma-Aldrich), equilibrated with 1x DPBS using a syringe pump at a flow rate of 0.05 ml/min. The eluted colored fractions consisting of BPD-PC-containing Cet-Pz-N_3 and Cet-PEG_4-N_3 PINs were collected and stored in the dark at 4°C. The molar concentration of nanoconstructs was calculated using the molar concentration of lipid within a typical formulation (34.043 mM) and the approximation that a unilaminar nanovesicle with a hydrodynamic diameter of 100 nm is formed of 80,000 lipids, based on the following equation.[6]

$$N_{tot} = \frac{\left[4\pi \left(\frac{d}{2}\right)^2 + 4\pi \left(\frac{d}{2} - h\right)^2\right]}{a}$$

N_{tot} is the total number of lipids per nanovesicle, d is the hydrodynamic diameter in nanometers and h is the thickness of the bilayer in nanometers, which approximates to 5 nm. For a phosphatidylcholine nanoconstruct preparation such as the one used in this study, this equation can be simplified further to the following equation.

$$N_{tot} = 17.69 \times \left[\left(\frac{d}{2}\right)^2 + \left(\frac{d}{2} - 5\right)^2\right]$$

Once the total number of lipids per nanoconstruct was obtained, the molar concentration of nanoconstruct was derived and used for approximating the quantities of Cet-Pz-N_3 and Cet-PEG_4-N_3 conjugated. The concentration of the BPD-PC within the PIN formulations was determined using UV-Visible absorption spectroscopy ($\varepsilon_{687\ nm}$ = 34,895 $M^{-1}.cm^{-1}$) in DMSO dilutions. The degree of conjugation of Cet-Pz-N_3 and Cet-PEG_4-N_3 to the PINs was determined using fluorimetry with standard curves of free antibodies in 1x DPBS generated using $Exc_{480\ nm}/Emi_{521\ nm}$ (5-FAM on the Cet-Pz-N_3) or $Exc_{480\ nm}/Emi_{517\ nm}$ (AF488 on the Cet-PEG_4-N_3) and an integration time of 0.1 s. Fluorescence emission of 1xDPBS dilutions (100-200-fold) of each purified Cet-Pz-N_3 and Cet-

PEG_4-N_3 PINs, were normalized to the BPD-PC concentration within each preparation. The autofluorescence of BPD-PC nanoconstructs not conjugated to antibodies was obtained under the same excitation parameters and the autofluorescence emission was normalized to the BPD-PC concentrations. This normalized autofluorescence was subtracted from the normalized fluorescence of Cet-Pz-N_3 and Cet-PEG_4-N_3 PINs. The Cet-Pz-N_3 and Cet-PEG_4-N_3 standard curves were used to derive the molar concentrations of the Cet click-conjugated to the PINs. The normalized molar concentrations of the click-conjugated Cet-Pz-N_3 and Cet-PEG_4-N_3 were used to derive the absolute number of antibodies conjugated to each nanoconstruct and the respective degree of conjugation.

Chemotherapy-loaded Cet-PINs: Cet-PINs conjugated to Cet-PEG_4-N_3 molecules were fabricated as described above, with slight modifications to the fabrication process. The lipid films were doped with 100 nmoles of 16:0 BPD-PC and were hydrated in 1ml of either gemcitabine hydrochloride (15 mg/ml; LC Labs), Oxaliplatin (7.5 mg/ml; SelleckChem) or 5-fluorouracil (10 mg/ml; Sigma-Aldrich). Following extrusion using 200 nm polycarbonate membranes, all liposomes were purified from unencapsulated chemotherapy using Sepharose CL-4B columns equilibrated with PBS. Purified liposomes were conjugated to Cet-PEG_4-N_3 as described above and purified once more after 24 h conjugation. Encapsulated chemotherapy was quantified using Agilent 6430 Triple Quad LC-MS/MS (oxaliplatin: 397 m/z precursor, 344 m/z product ion, 75 fragmentor, 15 collision energy, 7 accelerator voltage, positive ion mode; gemcitabine hydrochloride: 264 m/z precursor, 112 m/z product ion, 75 fragmentor, 15 collision energy, 7 accelerator voltage, positive ion mode; 5-fluorouracil: 129 m/z precursor, 42 m/z product ion, 90 fragmentor, 20 collision energy, 7 accelerator voltage, negative ion mode.)

Cell Culture: All cells were cultured in Corning® T75 cell culture flasks (Corning™). DMEM media supplemented with 1x Penicillin/Streptomycin and 10% heat-inactivated fetal bovine serum (FBS, Gibco) was used to culture A431 cells (ATCC) and MIA PaCa-2 cells (ATCC). RPMI media with glutamine supplemented with 1x Penicillin/Streptomycin and 10% heat-inactivated FBS was used to culture OVCAR-5 cells (NIH) and T47D cells (ATCC). CHO-WT and CHO-EGFR cells were kindly provided by Dr. T. Heitner at the Department of Anesthesiology, UCSF, San Francisco, California,[7] and were cultured in Ham's F12k media supplemented with 1x Penicillin/Streptomycin and 10% heat-inactivated FBS. CHO-EGFR cells were selected prior to use by supplementing the media with G-418 (0.8 mg/ml; Sigma Aldrich), which was removed two passages before molecular targeted NIR photodynamic activation of the cells. Cells were passaged by trypsinization using 0.05% Trypsin (Corning®).

Flow Cytometry Analyses: Confluent cells grown in monolayer in Corning® T75 cell culture flasks (Corning™) were washed once with 5 ml of 1x DPBS (without calcium or magnesium, Corning®) and once with 2 ml of 0.05% Trypsin (Corning®). The cells were then incubated at 37°C for a maximum of 3 min with mild agitation every 1 min. The detached cell suspensions were collected in media containing 10% FBS and centrifuged for 5 min at 1,000 xg, the supernatant was aspirated and discarded, and the cells were redispersed in their respective culture media containing 10% FBS. Following 40 repeated 10 ml pipette agitations to prepare single-cell suspensions, the cells were counted using a Coulter counter and 50,000 cells were placed into 1.5 ml microcentrifuge tubes. The cells were pelleted by centrifugation for 5 min at 1,000 xg, the media in the supernatant was discarded and replaced with 100 µl of the respective serum-containing culture media containing the PIN formulations (250 nM BPD equivalent). It must be noted that in the serum IgG concentration is 1.9mg/ml in the final PIN dilutions prepared in media containing

10% FBS.[8] Following 10 repeated pipette agitations to prepare single-cell suspensions, the cells were incubated at 37°C for 15 min in the dark. The cells were then pelleted again by centrifugation for 5 min at 1,000 xg, the media containing the PIN formulations in the supernatant was discarded and replaced with 200 µl 1x DPBS (without calcium or magnesium, Corning®) and cooled to 4°C. Following 10 pipette agitations to prepare single-cell suspensions, the cells in 1x DPBS were transferred to flow cytometry tubes and temporarily stored on ice in the dark. For each condition, 10, 000 cells were analyzed using a BD FACSAria™ II flow cytometer (BD Biosciences®). Fluorescence of cell-associated BPD-PC was measured using a 405 nm laser, a 610 nm dichroic long pass filter and a simultaneous 620 nm long pass filter. Fluorescence of the 5-FAM and the Alexa Fluor® 488 were measured using a 405 nm laser and a 450/40 nm filter. When blocking with a cetuximab concentration that matches free IgG, 1 mg/ml of cetuximab was used and the final concentration of FBS was made to 5%, which equates to a final mean IgG concentration of 0.95 mg/ml that serves as an irrelevant antibody sham control throughout all in vitro experiments.[8] A control for competitive inhibition was also performed using a human IgG isotype control (Pierce).

Physical characterization of PINs: Z-average diameters, polydispersity indices and ζ-potentials of PINs were measured using a Zetasizer Nano ZS (Malvern Instruments Ltd.). For simultaneous z-average diameter and polydispersity index measurements, 2 µl of PINs were placed in a 4 ml polystyrene 4xOptical cuvette (Sarstedt AG & Co.) and 1 ml of 1x DPBS was added to the PINs. Temperature equilibration (120 s) was completed prior to the three individual measurements performed for each sample. ζ potential measurements were performed using a Folded Zeta Capillary Cell (Malvern Instruments Ltd.). 10 µl of PINs were diluted with 1 ml of 3 mM NaCl, loaded into the cell and three individual measurements were performed for each sample.

Cellular uptake studies: OVCAR-5 cells were trypsinized and seeded onto NUNC™ treated, black-walled, transparent base 96 well plates (Thermo Fisher Scientific) at a density of 50,000 cells per well for 24 h. PIN dilutions (250 nM BPD equivalent) prepared in RPMI media containing 10% FBS were added to the cells and incubated at 37°C. At the required time-points, the media containing PINs was aspirated from the wells and the cells were washed three times with 100 µl 1x DPBS (without calcium or magnesium, Corning®). Finally, the cells were digested in 50 µl Solvable™ (PerkinElmer) tissue digestion solution, the BPD equivalent fluorescence was measured using a plate reader (SpectraMAX M5), and the BPD equivalent concentration was determined using standard curves prepared in Solvable™. The protein concentration in each respective well was then measured using the Pierce BCA Protein Quantitation Kit (Thermo Fisher Scientific) and the BPD equivalent concentration was normalized to protein concentration for each well.

Confocal microscopy: OVCAR-5 cells were trypsinized and seeded onto glass bottom, black-walled 96 well plates (Thermo Fisher Scientific) at a density of 5,000 cells per well. PIN dilutions (250 nM BPD-PC equivalent) were prepared in RPMI media containing 10% FBS and were incubated for 6h or 24h at 37°C. Hoechst® 33342 or LysoTracker® Red DND-99 (Thermo Fisher Scientific) were added to the cells according to the manufacturers protocols. The nuclei were visualized with the Hoechst stain (405 nm laser), the PINs were visualized using the BPD-PC fluorescence (405 nm laser) and the lysosomes were visualized using the LysoTracker (488 nm laser). For visual clarity, all blue channel images were uniformly set to 1-100, red channel images were uniformly set to 6-40, and green channel images were uniformly set to 1-80. All quantitative image analyses of colocalization were performed using unmodified images. Colocalization analysis of the BPD-PC-containing PINs and the lysosome-specific LysoTracker® marker was

performed using confocal microscopy and a subsequent custom-developed Matlab routine to analyze the images. The imaging was performed using a confocal microscope (Olympus FV1000) through a 60X objective (1.2NA, Water). For each field of view, a bright-field image and fluorescence images were acquired simultaneously. Image analysis initially highlighting each group of cells from the bright-field image. Then, the fluorescence images were binarized using a threshold defined by control images of untreated cells. Finally, for each object identified on the bright-field image, pixels exhibiting signals in both the BPD-PC channel and the LysoTracker® channel were counted and converted into a metric termed 'colocalization area'. The ratio of photosensitizer colocalized with the LysoTracker® was calculated by dividing this colocalization area by the total area occupied by the BPD-PC nanoconstructs.

Molecular targeted NIR photoactivation in 2D cells: At 60-80% confluence, A431 cells, OVCAR-5 cells, T47D cells and MIA PaCa-2 cells were seeded onto NUNC™ treated, black-walled, transparent base 96 well plates (Thermo Fisher Scientific) at a density of 1,500 cells per well 24 h before treatment. CHO-WT and CHO-EGFR cells were seeded onto the same 96 well plate type at a density of 400 cells/well 24h prior to experimentation. PIN dilutions prepared in the respective FBS-containing cell culture media were prepared and incubated with cells for 6h at 37°C. The PINs were then removed from the cells, replaced with fresh respective FBS-containing cell culture media and irradiated using an Intense 7401 690 nm laser with a fluence of 20 J/cm^2 at an irradiance of 150 mW/cm^2. Irradiance was measured using a Vega Handheld Power Meter (Ophir). Following molecular targeted NIR photoactivation, the cells were incubated for 72 h prior to assessing the viability. The media was removed from the cells and replaced with fresh respective FBS-containing cell culture media containing 3-(4,5-Dimethylthiazol-2-yl)-2,5-Diphenyltetrazolium Bromide (MTT, 0.1 mg/ml; Sigma-Aldrich) and incubated for 1 h at 37°C

(T47D cells were incubated for 1.5h). The media containing MTT was then removed from the cells, the formazan was dissolved in DMSO and the absorbance was measured at 517 nm. Viability was calculated as a percentage absorbance at 517 nm with respect to untreated control cells.

Cet-PIN selectivity and penetration in monotypic and heterotypic PDAC organoids: Fluorescent Cet-PIN constructs were prepared as previously described without doping of 16:0 BPD-PC. The DSPE-PEG lipid content was modified to incorporate an amino terminal lipid for fluorophore conjugation as such; DSPE-mPEG$_{2000}$ (4.3 mol%), DSPE-PEG$_{2000}$-DBCO (0.5 mol%) and DSPE-PEG$_{2000}$-NH$_2$ (0.2 mol%). Lipid films were prepared and hydrated in 1xDPBS as described earlier. Alexa Fluor® 680 NHS ester was reacted with the PINs at a 5-fold molar excess to DSPE-PEG$_{2000}$-NH$_2$ for 24 h at room temperature. Unreacted Alexa Fluor® 680 was removed by dialysis against 1x PBS in 100 kDa Float-A-Lyzer® dialysis tubes (Spectrum Labs) at 4°C for 48 h. Cet-PEG$_4$-N$_3$ was reacted with the nanoconstructs as described earlier to prepare Cet-PINs, which were then purified using Sepharose CL-4B size exclusion chromatography equilibrated with 1x DPBS. Untargeted Alexa Fluor® 680 tagged nanoconstructs were prepared as a control. Lipid content was quantified by back calculation from the Alexa Fluor® 680 concentration that was determined using UV-visible spectrophotometry and an extinction coefficient $\varepsilon_{694\ nm}$ = 182,000 $M^{-1}.cm^{-1}$. The same procedure was used to generate Cet-PIN-IRDye800 constructs for photoacoustic imaging.

MIA PaCa-2 cells (2,500 cells per well) were cultured in DMEM with 10% FBS for 48 h in Corning® Costar® Ultra-Low attachment 96 well plates in the absence or presence of patient-derived Pancreatic Cancer-Associated Fibroblasts[9] (PCAF; 2,500 cells per well). The PCAF cells were a kind gift from Dr. Diane Simeone. Organoids were then incubated with 42.55 μM lipid equivalent of Cet-PINs and untargeted constructs labeled with Alexa Fluor® 680 in DMEM containing 10% FBS for 1, 6 or 24h, followed by three 100 μl washes in culture medium. The

organoids were then fixed with 10% formalin for 10 min, followed by three 100 µl washes in 1M glycine before confocal microscopy imaging.

To quantify the Cet-PIN specificity, the organoids were imaged using a 10x objective and a 635 nm laser with the highest acquisition parameter threshold set to the highest signal coming from organoids incubated with the Cet-PIN-Alexa680 at each time-point, across all the organoids. Z-stack images across a 75 µm cross-section of the organoids were acquired, projected as sum of intensities of all images in the z-stack using ImageJ software and saved as tiff files for quantification. The tiffs (brightfield and fluorescence images) were processed in Matlab (Mathworks Inc) using custom written segmentation-based algorithms[10] to deduce PIN intensity as a function of organoid area. The sum of intensities/pixel for the Cet-PIN-treated organoids was divided by the intensity of the organoids incubated with the untargeted constructs to obtain normalized metrics for targeting specificity.

To visualize PIN penetration, the organoids were imaged using two-photon microscopy with a 40x objective and 800 nm excitation using a Mai Tai Laser. Acquisition was standardized to each individual organoid. Z-stack images across a 100 µm cross-section of the organoids were acquired and projected in three-dimensional space using AMIRA (FEI Inc) 3D reconstruction software and customized color bars to display the organoids from different treatment groups. 2D cross-sections of the middle 50% Z-plane of each organoid was selected to evaluate the degree of organoid penetration.

NIR photodynamic activation in monotypic and heterotypic organoids, and CALYPSO image analysis for viability: MIA PaCa-2 monotypic organoids and MIA PaCa-2 – PCAF heterotypic organoids were prepared as described. 48h after seeding, the organoids were incubated with varying concentrations of BPD equivalent of Cet-PINs and untargeted constructs for 6h, followed

by three 100 μl washes in culture medium. Organoids were then subject to 40 J/cm^2 of 690 nm laser light at an irradiance of 150 mW/cm^2. 72h following molecular targeted NIR photoactivation, the LIVE/DEAD Cell Viability reagent mixture was added to each organoid according to the manufacturer's protocol (Thermo Fisher Scientific) and the organoids were imaged using confocal microscopy. Images were analyzed using the previously reported Comprehensive high-throughput image analysis for quantifying the therapeutic efficacy in architecturally complex heterotypic organoids (CALYPSO).[11] Untreated control organoids were used for thresholding of viability signals and total killing control organoids (formalin fixation, Triton X-100 permeabilization) were used for thresholding of dead cell signals. CALYPSO analysis generated viability heatmap images and empirical outputs of fractional viability. All treatment conditions were performed with an *n* of 4-8 organoids. For Cet-PINs encapsulating chemotherapy, heterotypic organoids were incubated with 1 μM and 2 μM BPD-PC equivalent of constructs for 6 h 24 h after seeding, prior to NIR photodynamic activation with 40 J/cm^2 of 690 nm laser light at an irradiance of 150 mW/cm^2. 72h following treatment, CALYPSO analysis was performed as described above.

In vivo Cet-PIN penetration and molecular targeted NIR photodynamic activation: Swiss nude mice were purchased from Cox7 at Massachusetts General Hospital. Subcutaneous heterotypic MIA Paca-2 + PCAF tumors were generating by implantation of a mixture of 1 x10^6 cells of each cell line in 50 μl of culture media and Matrigel (50% v/v). When the tumors reached ~50mm^3, they were imaged using photoacoustic imaging (PAI) to generate baseline images of tumor vascularity. The same mice were then intravenously injected with 5 nmol IRDye 800CW equivalent of Cet-PIN-IRdye800 constructs. 12 hours following administration, the tumors were imaged using PAI to generate 2D cross sections and 3D render images of the Cet-PIN penetration out of the vessels within the tumor.

For *in vivo* molecular targeted NIR photodynamic activation, mice were implanted with heterotypic MIA Paca-2 + PCAF tumors as described above. Cet-PIN constructs or untargeted constructs were administered *via* tail vein injection to the mice at a dose of 0.5 mg/kg BPD equivalent. 12 h following administration, the tumors were illuminated with NIR light for *in vivo* photodynamic activation of the constructs (690 nm, 150 J/cm^2, 100 mW/cm^2). Tumors were harvested 72 h following molecular targeted and untargeted NIR photodynamic activation for histological analysis. The overlying skin, vicinal muscle, proximal liver and photodamaged bowel was also harvested for histological analysis. Tumors and tissue were cryosectioned and stained with hematoxylin and eosin (H&E) stains. Tumors cryosections were also stained with Masson's trichrome stain to visualize collagen. For visual clarity only, all images were evenly set to (0.8 Gamma, 136% brightness, 155% contrast, 72% red, 102% green, 102% blue.) Tumor necrosis and collagen in stained tumor slices were quantified from unaltered, as-acquired images using custom-developed Matlab routines. Whole slide TIFF images obtained from the Nanozoomer imaging system were quantified using custom designed Matlab routines as previously described in detail by our group[12]. Specifically, the brightfield color images obtained from Nanozoomer imaging system were converted to gray scale and an Otsu threshold algorithm was used to identify tissue section boundaries to calculate the tumor cross section areas. The colored brightfield image was also analyzed via K space cluster analysis to isolate the tumor tissue stained areas (colored) from necrotic zones (no color). A ratio of area of tumor tissue necrosis to total tumor cross-section area provided % necrosis per tumor cross-section.

SUPPLIMENTARY RESULTS

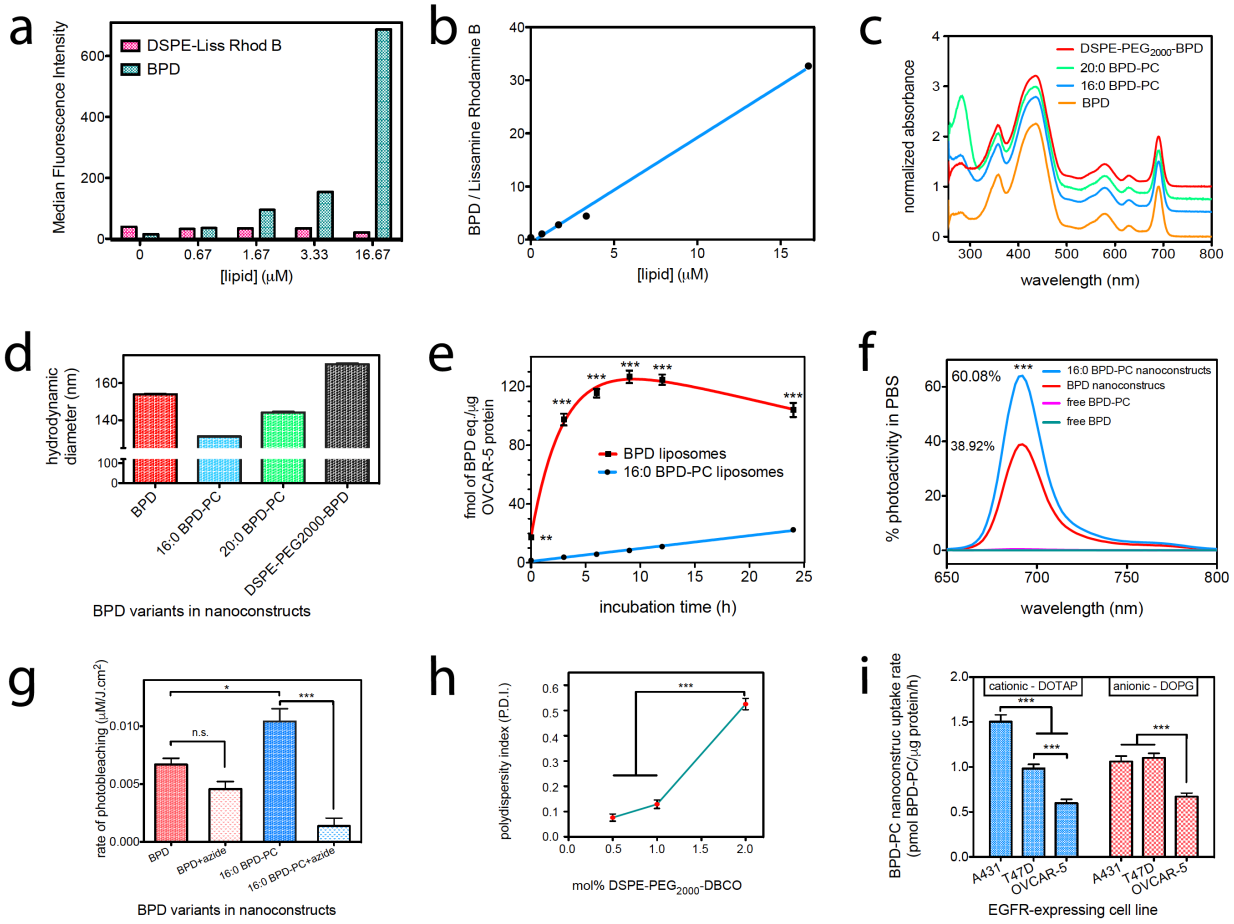

Figure S1. a) Median florescence intensities of BPD and DSPE-Lissamine Rhodamine B (DSPE-Liss Rhod B) in OVCAR-5 cells incubated for 30 min with increasing lipid concentration equivalents of nanconstructs co-doped with BPD and the lipid anchored fluorophore DSPE-Liss Rhod B. b) A concentration-dependent increase in the BPD/Liss Rhod B ratio confirms that BPD leeches from the nanoconstruct liposomal bilayer into the cells. c) Normalized UV-Visible absorption spectra of free BPD and its lipidated variants DSPE-PEG_{2000}-BPD, 20:0 BPD-PC and 16:0 BPD-PC diluted in DMSO confirm that no spectral shift of the photosensitizer occurs after conjugation to the lipids. The spectra are off-set by 0.25 for clarity. d) Hydrodynamic diameters of nanoconstructs formulated with BPD and its lipidated variants, demonstrating average diameters of 130-150 nm, whereas the DSPE-PEG_{2000}-BPD doped nanoconstructs exhibit a larger

diameter of ~170 nm. e) 16:0 and 20:0 lyso PC anchoring of BPD into nanoconstructs prevents the non-specific uptake of BPD into OVCAR-5 cells over 24h. f) 16:0 BPD-PC nanoconstructs exhibit 21% greater fluorescence activity than BPD nanoconstructs and g) a 36% faster rate of photobleaching that is reduced in the presence of the singlet oxygen quencher sodium azide. h) polydispersity indices (P.D.I.s) measurements of BPD-PC nanoconstructs containing 5 mol% DSPE-mPEG$_{2000}$ with incremental increases in DSPE-PEG$_{2000}$-DBCO composition reveal an instability with 2 mol% DSPE-PEG$_{2000}$-DBCO. i) Uptake rates of cationic (DOTAP) and anionic (DOPG) BPD-PC nanoconstructs in EGFR-expressing cell lines (A431 high, T47D low, OVCAR-5 high). (Mean ± S.E.M., One-Way ANOVA with a Tukey Post-Test.)

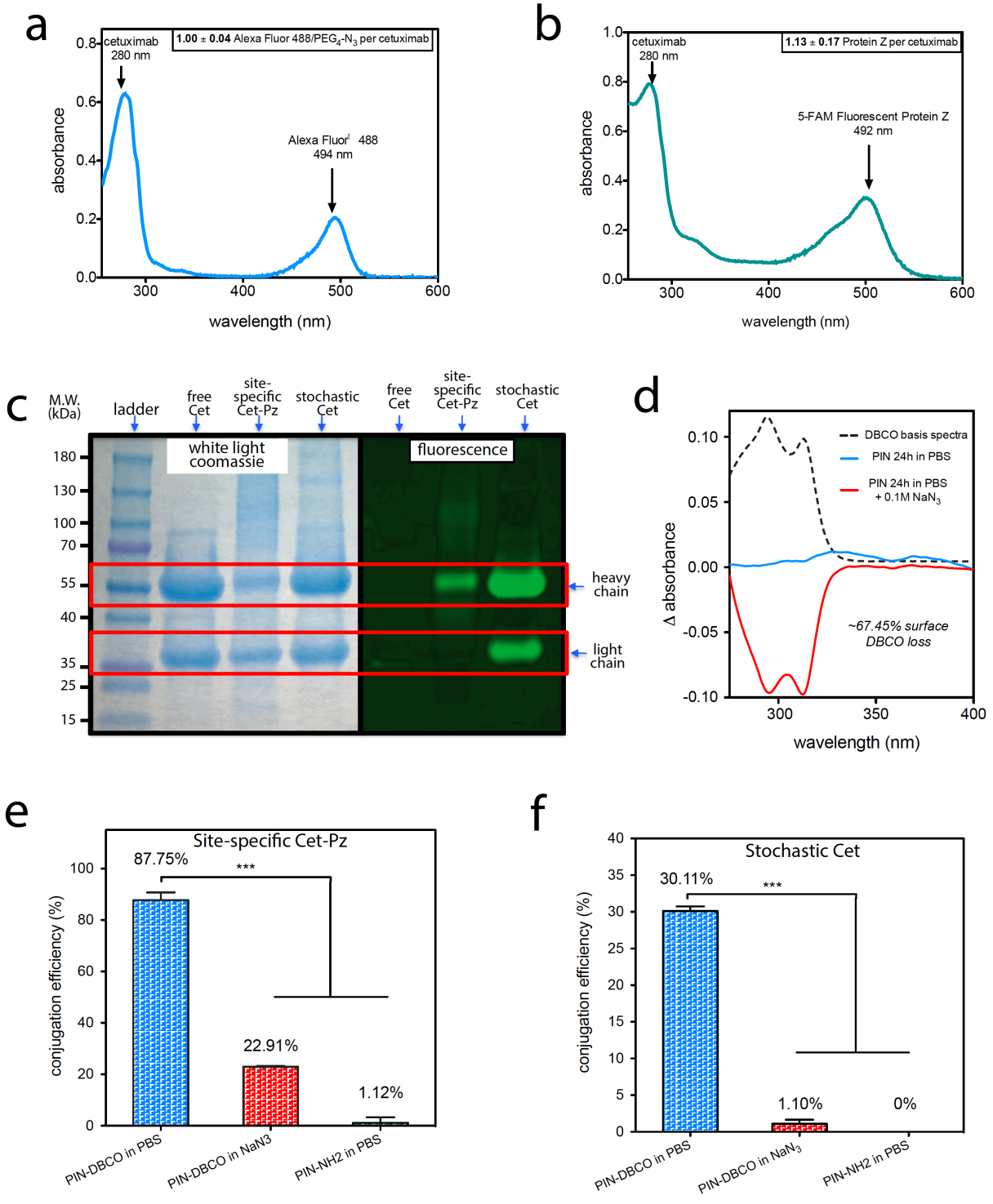

Figure S2. UV-visible absorption spectra of cetuximab site-specifically modified with a single Protein Z molecule, fluorescently labeled with 5-FAM (a) or stochastically modified with a single Alexa Fluor® 488 and single PEG_4-N_3 linker (b). c) Denaturing sodium dodecyl sulfate

polyacrylamide gel electrophoresis (SDS-PAGE) analysis of free cetuximab, cetuximab conjugated to protein Z, and cetuximab conjugate to Alexa Fluor® 488 and PEG_4-N_3. Coomassie blue stain (GelCodeTM Blue Safe Protein Stain, left) shows the heavy chains and light chains of cetuximab following the denaturing electrophoresis. Fluorescence imaging of the gels reveals 5-FAM fluorescence only from the heavy chain of the site-specific Protein Z conjugate, and Alexa Fluor® 488 fluorescence from both the heavy and light chains of the stochastic conjugate. Inactivation of 67.45% of the nanoconstruct's surface DBCO using 0.1M NaN_3 (d) significantly reduces the conjugation efficiency of site-specific Cet-Pz (e) and stochastic Cet (f). Adsorption of either Cet-Pz or Cet to BPD-PC nanoconstructs void of DBCO is negligible. (Mean ± S.E.M., One-Way ANOVA with a Tukey Post-Test.)

Table S1. Physical characterization of PINs conjugated to site-specific Cet-Pz and stochastic Cet-PEG_4-N_3 at varying lipid : Cet mass ratios.

Conjugation Strategy	Lipid: Cet Mass Ratio	*Z*-average Diameter [a]	P.D.I. [b]	ζ-potential [c]	Cet per PIN	Cet surface density [d]
	1:0	138.1 (±7.2)	0.144 (±0.03)	-23.6 (±0.5)	0	0
Cet-Pz	1:0.02	151.4 (±7.6)	0.134 (±0.03)	-22.6 (±0.4)	13.8 (±2.2)	191.6 (±30.6)
	1:0.05	161.9 (±24.0)	0.147 (±0.03)	-22.7 (±0.5)	31.3 (±3.2)	380.1 (±38.9)
	1:0.10	161.0 (±23.0)	0.156 (±0.07)	-21.7 (±0.6)	61.9 (±5.1)	760.1 (±62.6)
	1:0.15	164.6 (±22.5)	0.171 (±0.03)	-21.0 (±1.0)	84.7 (±7.4)	995.1 (±86.9)
	1:0.20	167.9 (±13.1)	0.165 (±0.01)	-19.8 (±1.0)	100.0 (±5.9)	1129.14 (±66.6)
Cet-PEG_4-N_3	1:0.02	138.0 (±16.2)	0.135 (±0.05)	-22.9 (±0.8)	4.2 (±1.0)	70.2 (±16.7)
	1:0.05	145.7 (±24.0)	0.139 (±0.04)	-22.5 (±0.6)	8.6 (±3.5)	129.0 (±52.5)
	1:0.10	157.0 (±30.8)	0.214 (±0.10)	-21.9 (±0.9)	18.0 (±6.4)	232.5 (±82.6)
	1:0.15	134.8 (±4.0)	0.097 (±0.00)	-20.1 (±1.8)	23.1 (±4.3)	404.7 (±75.3)
	1:0.20	134.7 (±11.0)	0.092 (±0.06)	-20.5 (±0.7)	29.5 (±7.9)	517.5 (±138.6)

[a] nanometers (nm), [b] polydispersity index, [c] millivolts (mV), [d] Cet per μm^2.
Values are mean (± S.D.)

Table S2. Efficacy of molecular targeted NIR photodestruction in cells with varying degrees of EGFR expression using Cet-PINs and untargeted constructs, irradiated with 690 nm light (20 J/cm^2 at 150 mW/cm^2).

Cell Line	IC_{50} with untargeted construct [a]	IC_{50} with Cet-PINs [a]	Fold Reduction in IC_{50}	% IC_{50} of untargeted construct
MIA PaCa-2	271.4	9.3	32.7	3.4
OVCAR-5	548.7	70.9	8.3	12.9
A431	489.9	105.0	5.3	21.4
T47D	798.5	563.2	1.6	60.7
CHO-WT	3229.5	4649.8	0.8	144.0
CHO-EGFR	3717.7	5.4	760.8	0.1

[a] nanomolar (nM) BPD-PC equivalent. (mean values).

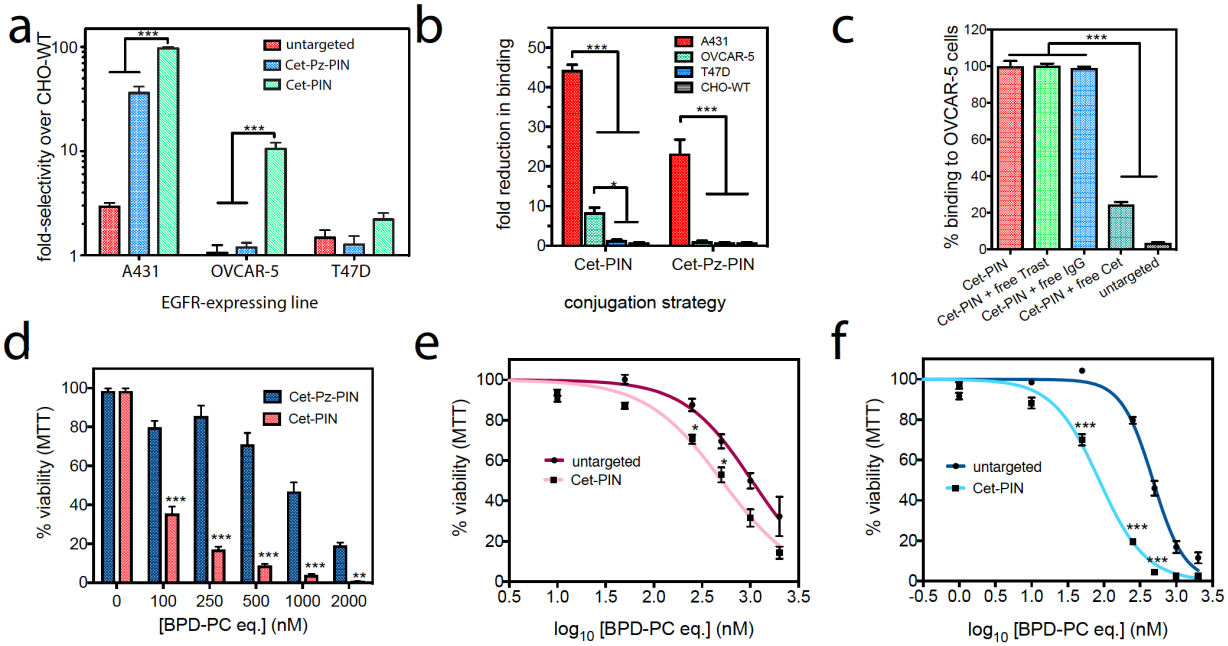

Figure S3. a) The binding selectivity of unconjugated construct, Cet-Pz-PIN and Cet-PIN to A431, OVCAR-5 and T47D cells are presented with respect to EGFR-null CHO-WT cells. b) Degree of reduction in binding of Cet-PIN and Cet-Pz-PIN constructs to A431, OVCAR-5, T47D and CHO-WT by the presence of 1 mg/ml free cetuximab that matches the concentration of free human IgG in the serum-containing media. c) Competitive inhibition of Cet-PIN binding to OVCAR-5 cells using 100x free Cet reduces PIN binding by 80%, yet binding is unaltered in the presence of 100x free Trastuzumab or free IgG sham. d) Difference in molecular targeted NIR photodestruction of OVCAR-5 cells treated with the Cet-PIN construct and the Cet-Pz PIN construct. Phototoxicity dose response curves of T47D (e) and A431 (f) cells treated with an untargeted construct and the optimal Cet-PIN construct. All values are mean ± S.E.M., One-Way ANOVA with a Tukey Post-Test.

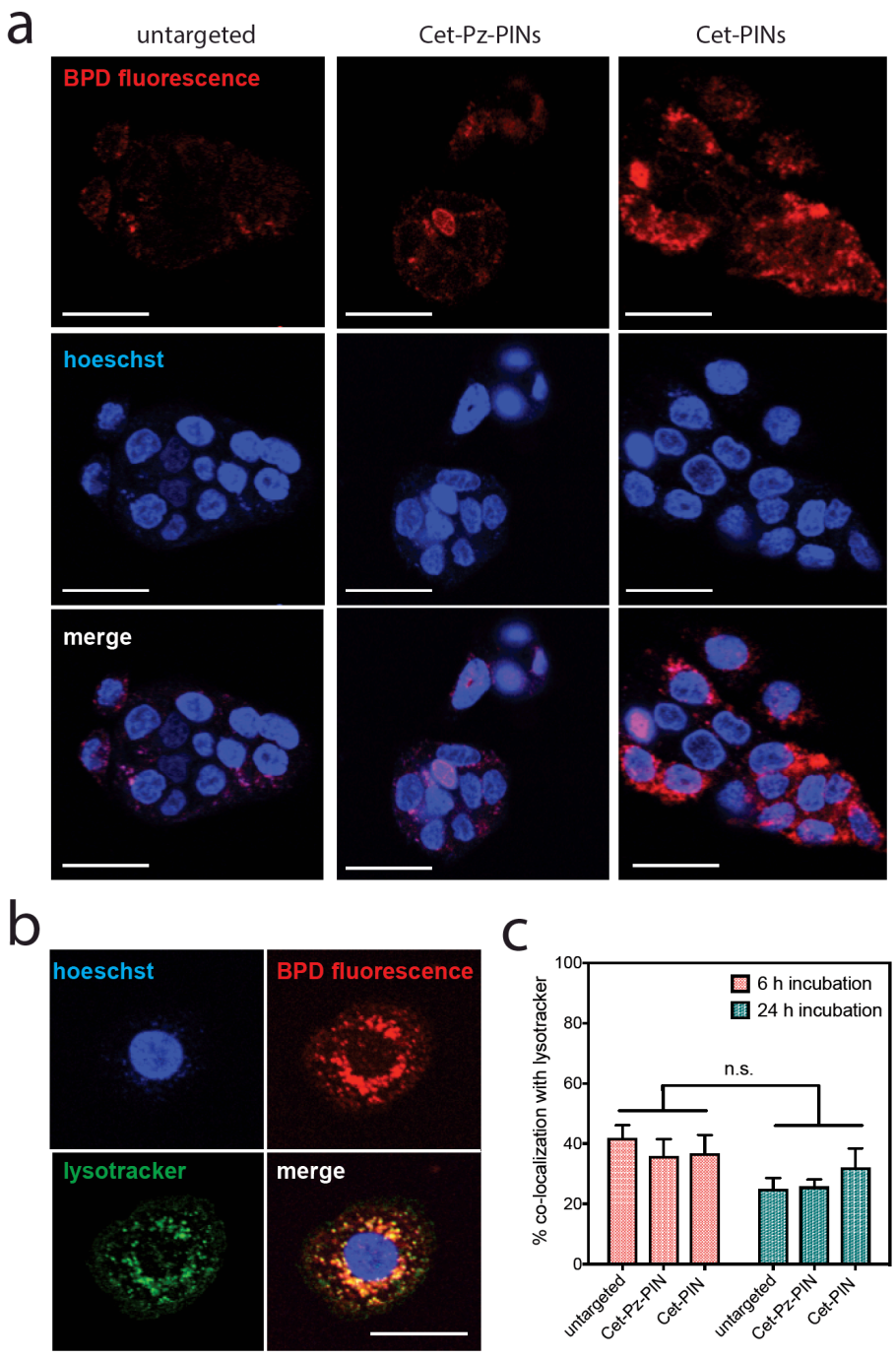

Figure S4. a) Confocal images (60x) of OVCAR-5 cells incubated for 6h with untargeted (left), Cet-Pz-PIN (center) and Cet-PIN (right) constructs. b) Visual lysosomal colocalization of Cet-PIN constructs in OVCAR-5 cells. (Scale bars are 50 μm) c) Quantification of lysosomal co-

localization of untargeted, Cet-Pz-PIN and Cet-PIN constructs at 6h and 24h incubation times. (mean ± S.E.M., n=8, One-Way ANOVA with a Tukey Post-Test.)

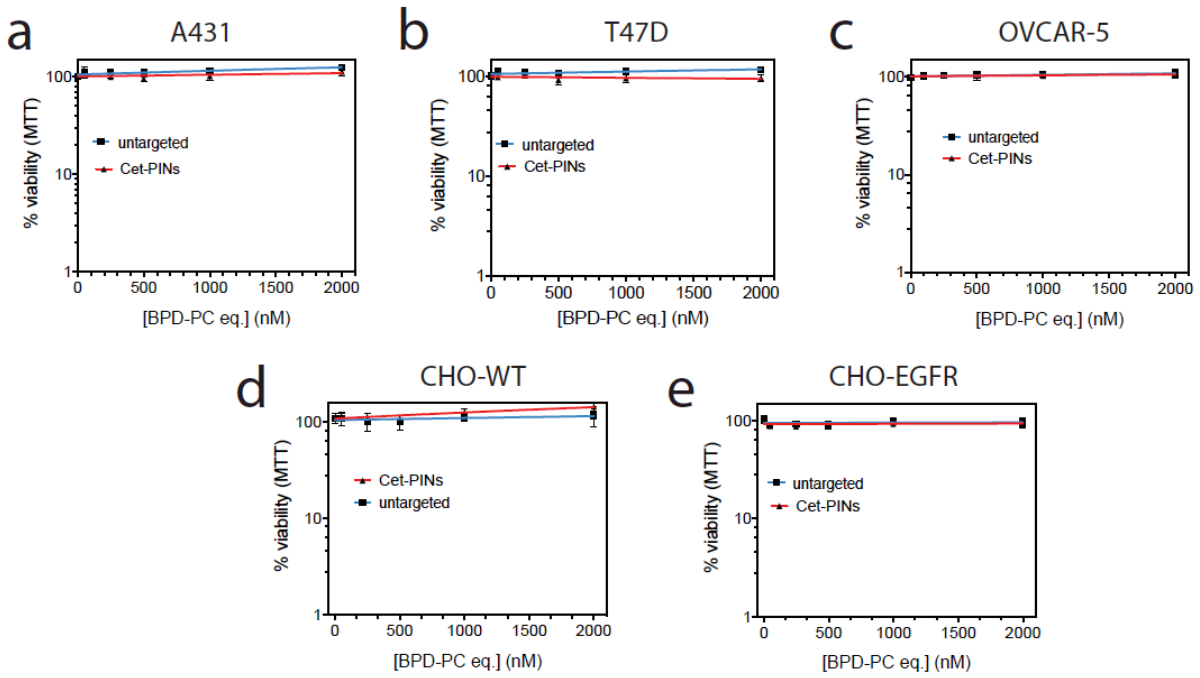

Figure S5. Absence of dark toxicity of untargeted constructs and the Cet-PINs in A431 (a), T47D (b), OVCAR-5 (c), CHO-WT (d) and CHO-EGFR cells (e) treated for a 6 h pulse, followed by 72 h incubation. Viability was measured using the MTT assay. (values are mean ± S.E.M.)

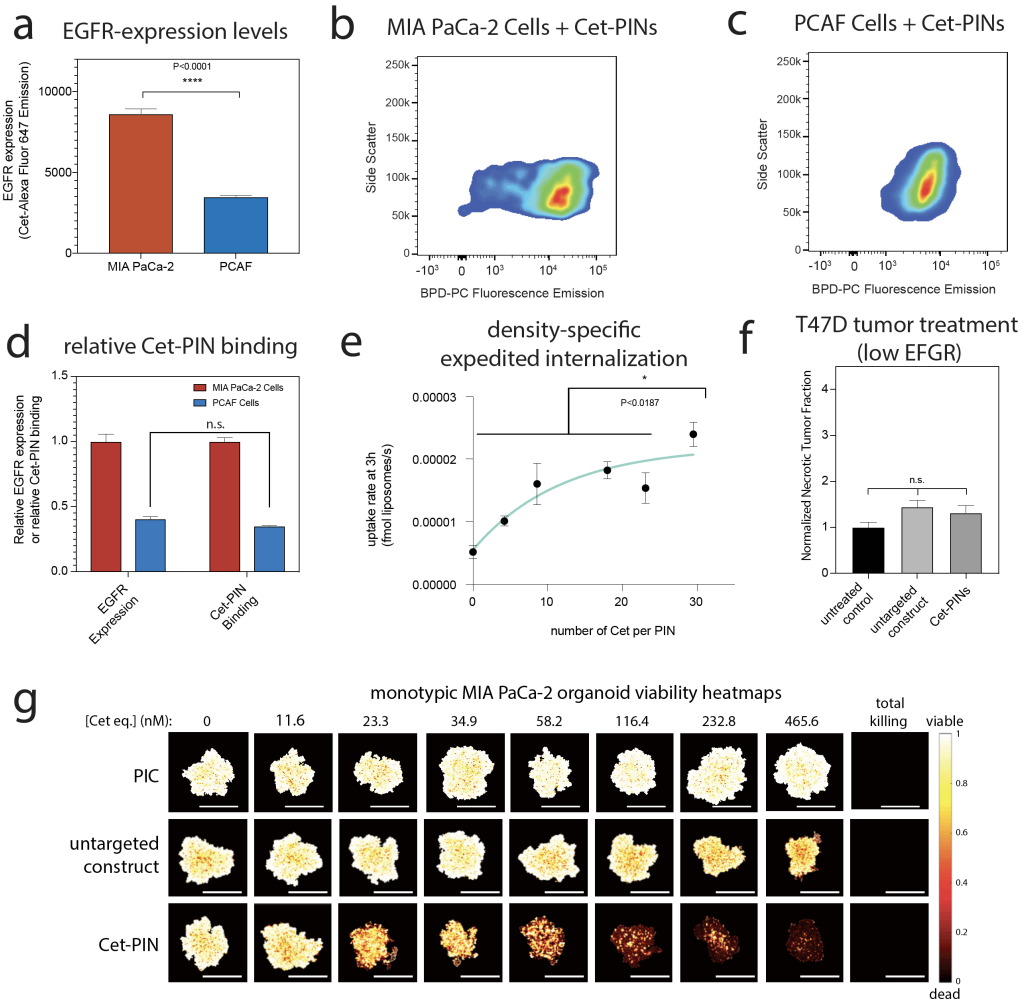

Figure S6. a) EGFR expression in MIA PaCa-2 cells and PCAF cells determined using flow cytometry, depicted as the median fluorescence emission of Alexa Fluor 647 conjugated to Cetuximab. Representative flow cytometry plots of MIA PaCa-2 cells (b) and PCAF (c) cells incubated with Cet-PINs. d) A comparison between relative EGFR expression levels in MIA PaCa-2 cells and PCAF cells with the relative binding of Cet-PINs to the two cell lines. e) Cet-PINs exhibit ligand-density specific expedition of cellular internalization rates in OVCAR-5 cells. f) Photodynamic activation of Cet-PINs and untargeted constructs does not induce tumor necrosis in low EGFR-expressing T47D tumors. g) Viability heatmap images of monotypic PDAC organoids following molecular targeted NIR photodynamic activation with increasing concentrations of PIC,

untargeted construct and the specificity-tuned Cet-PIN (mean ± S.E.M. and n=3 for a-d and f, n=4 for e and g, One-Way ANOVA with a Tukey Post-Test.)

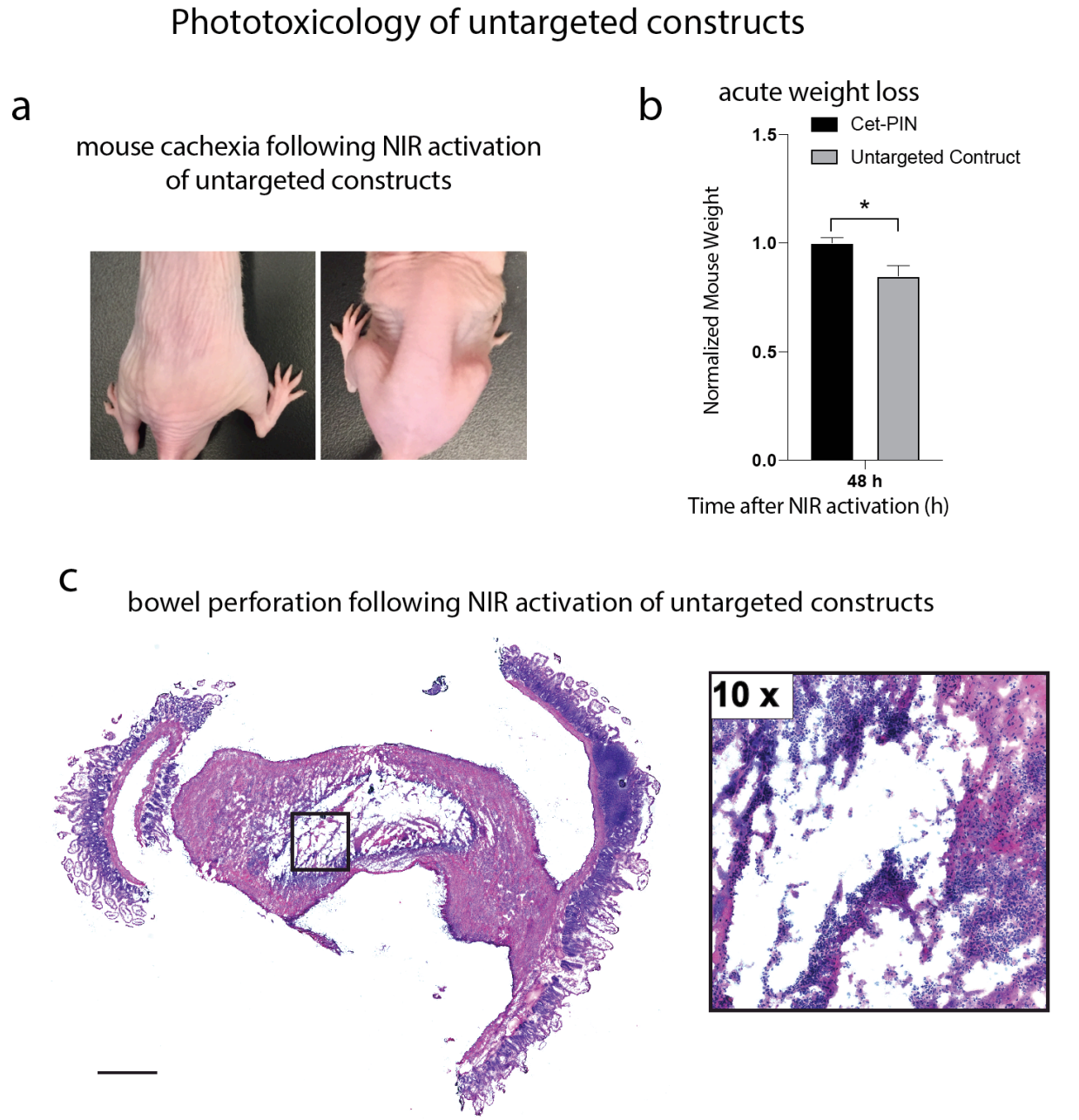

Figure S7. a) Representative photograph of mouse cachexia 72h following NIR photodynamic activation of untargeted constructs administered to mice bearing MIA PaCa-2 + PCAF heterotypic tumors (right), as compared to untreated mice (left). b) Acute weight loss of mice 72h following

NIR photodynamic activation of untargeted constructs, whereas untreated mice and mice treated with NIR photodynamic activation of Cet-PINs exhibited no change in body mass (two-tailed *t* test, * = P< 0.05). c) Bowel perforation evident from H&E stained tissue sections of visibly ulcerating bowel tissue 72h following NIR photodynamic activation of untargeted constructs administered to mice bearing MIA PaCa-2 + PCAF heterotypic tumors. (Scale bars is 1 mm.)

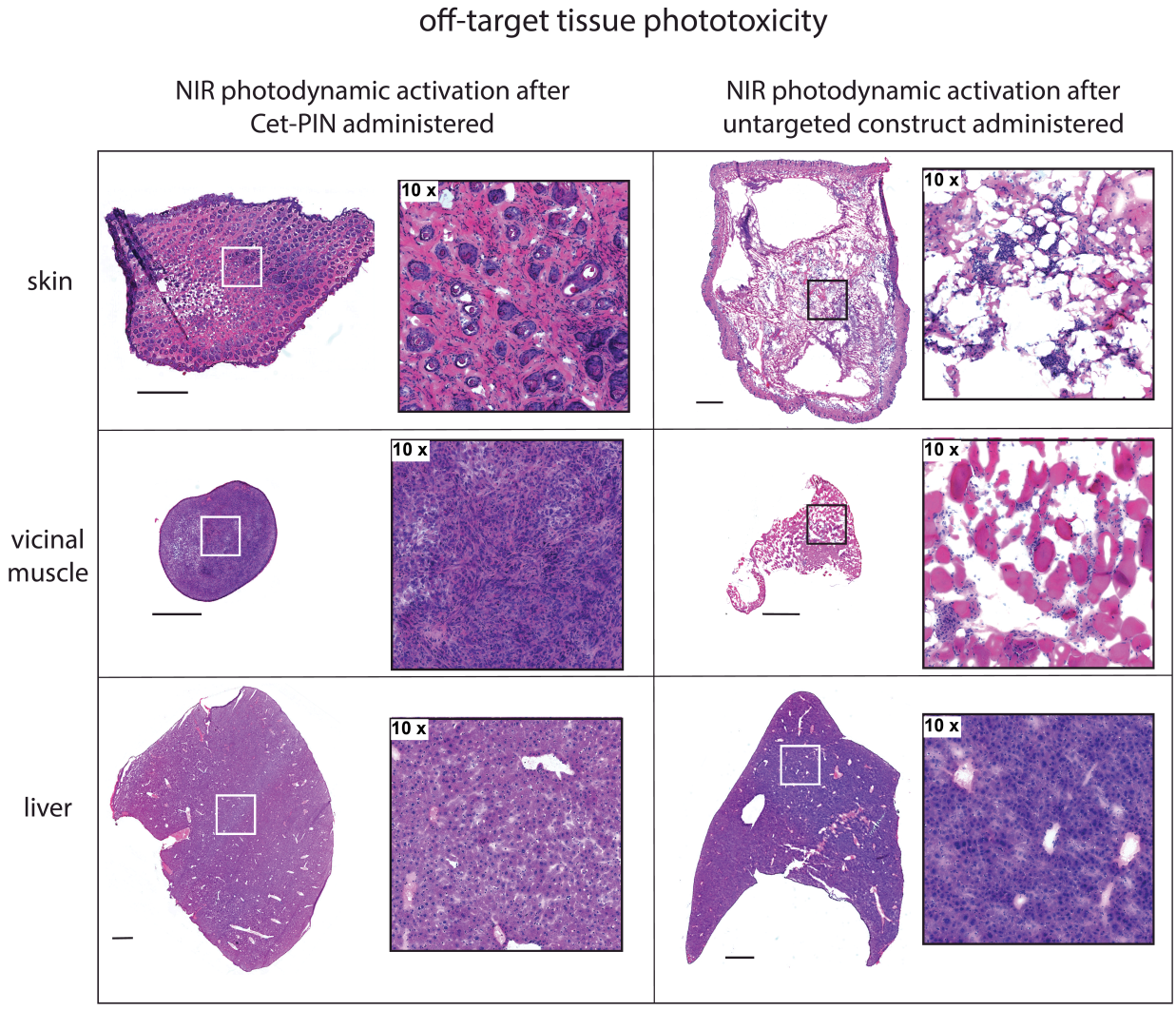

Figure S8. H&E stained tissue sections of skin directly covering MIA PaCa-2 + PCAF heterotypic tumors, vicinal muscle, and proximal liver tissue following NIR photodynamic activation of the specificity-tuned Cet-PINs or untargeted constructs. NIR photodynamic activation of untargeted

constructs induced significant tissue necrosis in skin covering the tumor and vicinal muscle, whereas NIR photodynamic activation of the Cet-PINs induced no off-target phototoxicity. The parts of the liver in close proximity to the site of NIR photodynamic activation was unaffected. Scale bars are 1mm.

REFERENCES

[1] R. Warden-Rothman, I. Caturegli, V. Popik, A. Tsourkas, *Anal. Chem.* **2013**, *85*, 11090-11097.
[2] J. Z. Hui, A. Tsourkas, *Bioconjug. Chem.* **2014**, *25*, 1709-1719.
[3] M. R. Wilkins, E. Gasteiger, A. Bairoch, J. C. Sanchez, K. L. Williams, R. D. Appel, D. F. Hochstrasser, *Methods Mol. Biol.* **1999**, *112*, 531-552.
[4] J. F. Lovell, C. S. Jin, E. Huynh, T. D. MacDonald, W. Cao, G. Zheng, *Angew. Chem., Int. Ed.* **2012**, *51*, 2429-2433.
[5] G. Obaid, W. Jin, S. Bano, D. Kessel, T. Hasan, *Photochem. Photobiol.* **2018**.
[6] aM. A. Jones, P. K. Kilpatrick, R. G. Carbonell, *Biotechnol. Prog.* **1993**, *9*, 242-258; bF. J. Hutchinson, S. E. Francis, I. G. Lyle, M. N. Jones, *Biochim. Biophys. Acta* **1989**, *978*, 17-24.
[7] T. Heitner, A. Moor, J. L. Garrison, C. Marks, T. Hasan, J. D. Marks, *J. Immunol. Methods* **2001**, *248*, 17-30.
[8] K. M. Morrill, H. D. Tyler, *Animal Industry Report* **2012**, *658*, 40.
[9] M. Waghray, M. Yalamanchili, M. Dziubinski, M. Zeinali, M. Erkkinen, H. Yang, K. A. Schradle, S. Urs, M. Pasca Di Magliano, T. H. Welling, P. L. Palmbos, E. V. Abel, V. Sahai, S. Nagrath, L. Wang, D. M. Simeone, *Cancer Discov.* **2016**, *6*, 886-899.
[10] aS. Mallidi, Z. Mai, I. Rizvi, J. Hempstead, S. Arnason, J. Celli, T. Hasan, *J. Biomed. Opt.* **2015**, *20*, 048003; bC. A. Schneider, W. S. Rasband, K. W. Eliceiri, *Nat. Methods* **2012**, *9*, 671-675.
[11] A. L. Bulin, M. Broekgaarden, T. Hasan, *Sci. Rep.* **2017**, *7*, 16645.
[12] S. Mallidi, Z. Mai, I. Rizvi, J. Hempstead, S. Arnason, J. P. Celli, T. Hasan, *J. Biomed. Opt.* **2015**, *20*, 048003.